Macromolecules
ARTICLE

Macromolecules **2010**, *43*, 1473–1479 **1473**
DOI: 10.1021/ma9024653

Basis of Solubility versus T_C Correlations in Polymeric Gas Separation Membranes

Nico F. A. van der Vegt,*,† Victor A. Kusuma,‡ and Benny D. Freeman‡

†*Center of Smart Interfaces, Technische Universität Darmstadt, D-64287 Darmstadt, Germany and*
‡*Department of Chemical Engineering, University of Texas at Austin, Austin, Texas 78712*

Received November 10, 2009; Revised Manuscript Received December 22, 2009

ABSTRACT: Gas molecules dissolve in dense rubbery matrices by occupying empty cavities created by thermal fluctuations in the matrix. In this paper, we describe the corresponding thermodynamics in terms of cavity formation and penetrant binding steps. We illustrate that the contributions of these processes to the sorption enthalpy can be estimated from experimental gas sorption and volume dilation data. A simple argument is provided to illustrate why the enthalpy change of cavity formation does not affect gas solubility, leaving behind the *binding enthalpy* as the relevant energy descriptor for penetrant sorption. The described procedure is accurate for systems in which the penetrant interacts with the polymer via dispersion forces and has been applied to analyze the solubility of hydrocarbons and perfluorocarbons in polydimethylsiloxane. Moreover, the two-step thermodynamic process for gas sorption considered in this work suggests a molecular basis of frequently observed correlations between gas solubility and gas critical temperature in rubbery and glassy polymers.

1. Thermodynamics of Penetrant Sorption

Gas and vapor solubility in polymeric membranes often correlate quite well with penetrant critical temperature, T_C. It is the purpose of this paper to discuss this correlation in terms of a microscopic view of gas sorption, which pictures dissolved penetrant molecules occupying molecular-sized gaps in the polymer and interacting with their surrounding polymer moieties through weakly attractive van der Waals forces. Correspondingly, we analyze the sorption enthalpy in terms of a "cavity formation" and a "penetrant binding" contribution and provide a simple, approximate route to extracting these contributions from experimental sorption and dilation data. These ideas are intended to provide the community of researchers working on developing polymeric gas separation membranes with a new means to relate gas/vapor solubility to molecular properties.

Solubility and Enthalpy of Penetrant Sorption. The thermodynamic treatment adopted here begins from the transfer free energy, ΔG_S (we use a subscript "S" for sorption), which describes the process of transferring one mole of penetrant molecules from the gas phase into the membrane. The relation to gas solubility, denoted S, is provided by[1]

$$S = \frac{T_0}{TP_0}\exp[-\Delta G_S/RT] \tag{1}$$

where R is the gas constant, T is the temperature, T_0 = 273.15 K, and P_0 = 1 atm. The transfer free energy can be resolved into enthalpic and entropic components according to the thermodynamic definition: $\Delta G_S = \Delta H_S - T\Delta S_S$. The enthalpy of gas sorption, ΔH_S, is usually obtained from temperature dependent solubility data using the expression[2]

$$S = S_0\exp[-\Delta H_S/RT] \tag{2}$$

where S_0 denotes a pre-exponential factor. ΔH_S is the change of the system's enthalpy corresponding to the thermodynamic process of dissolving one mole of penetrant gas and is usually interpreted as a measure of the strength of polymer-penetrant energetic interactions.

The enthalpy ΔH_S includes contributions resulting from the difference in cohesive forces operating between polymer segments before and after dissolving the penetrant as well as from cohesive van der Waals and electrostatic forces acting between the dissolved penetrant and the host polymer matrix.[3] Phrased differently, the sorption enthalpy includes a (matrix) reorganization contribution, ΔH_R, corresponding to the process of creating a molecular-sized gap (or cavity) in the polymer, and a penetrant binding contribution, ΔH_B, corresponding to the process of introducing the penetrant molecule in the preformed cavity (*cf.*, Figure 1)

$$\Delta H_S = \Delta H_R + \Delta H_B \tag{3}$$

In eq 3, ΔH_R is the *reorganization enthalpy*, and ΔH_B is the *binding enthalpy*. In contrast to a previous interpretation of ΔH_R by one of us,[1] we here interpret this quantity as the enthalpy of creating an empty cavity in the polymer. This interpretation holds only under the assumption that polymer-penetrant binding interactions provide a weak perturbation; i.e. cavities formed by thermal fluctuations of the liquid like matrix are not significantly perturbed by penetrant insertion. This interpretation is supported by recent theoretical and simulation studies.[4,5]

Although the above contributions to the enthalpy (eq 3) cannot be distinguished experimentally (heat does not come in different colors), theoretical arguments can be provided to permit their calculation to very good approximation. It is one of the purposes of this paper to provide an approximate expression for ΔH_R in terms of the thermo-physical properties of the polymer and the penetrant's partial molar volume. Since gas sorption at temperatures above the T_G of the polymer is thermodynamically equivalent to gas solubility in liquids, below we will refer to a "solute-solvent" system as an equivalent of a "penetrant-polymer" system.

*Corresponding author. E-mail: vandervegt@csi.tu-darmstadt.de.

Published on Web 01/07/2010

Enthalpy−Entropy compensation. The primary reason to introduce eq 3 and establish a route to estimate ΔH_R (and, thus, ΔH_B) is provided by a thermodynamic rule of *exact* enthalpy−entropy compensation[6−8]. This rule states that the free-energy ΔG_S ($=\Delta H_S - T\Delta S_S$) of solvating a solute in a liquid solvent is not affected by solvent reorganization; i.e., $\Delta H_R = T\Delta S_R$. Thus, ΔH_R and ΔS_R cancel in ΔG_S. The background of this compensation phenomenon is illustrated in Figure 2. Figure 2a shows a schematic representation of the configuration space of the solvent. Each point in this graph corresponds to a microstate (one of many possible arrangements of solvent molecules in the system) and the scribbly line shows a pathway along which the system explores these states in time. We will assume that the lighter gray area contains, e.g., 99.9% of all the relevant pure solvent microstates. We will, moreover, assume that this area includes a region (the darker gray area), corresponding to configurations shown in Figure 1, where the dashed stencil is devoid of solvent molecules (i.e., middle part of Figure 1). Because the enthalpy, when averaged over the microstates in this particular area only, exceeds the enthalpy averaged over all possible microstates by an amount ΔH_R, sampling this area in configuration space can be viewed to correspond with an enthalpy fluctuation, ΔH_R, of the liquid solvent. Because the system is at constant pressure and temperature, this enthalpy fluctuation involves heat exchange ($Q = \Delta H_R$) with the system's surroundings. From the second law of thermodynamics, the corresponding entropy fluctuation, ΔS_R, is given by $\Delta S_R = Q/T = \Delta H_R/T$, *i.e.*, $\Delta H_R = T\Delta S_R$. This phenomenon of exact enthalpy−entropy compensation is universal to all systems and inherent to any solvation process.[6] So far, we have only treated the first step in Figure 1, and we need to consider the solute insertion step to obtain the sorption entropy. Solute insertion results in confining the solvent's configuration space to the darker gray area as shown in Figure 2b. This confining effect reduces the configuration space of the solvent relative to that of the pure solvent and can be quantified with an "insertion probability", P_{ins}, whose exact definition has been discussed elsewhere.[9,10] Here it suffices to point out that solute insertion contributes a quantity $R \ln P_{ins}$ (which we refer to as the "excluded volume entropy") to the sorption entropy in addition to the contribution $\Delta H_R/T$. The sorption entropy corresponding to the combined process depicted in Figure 1 can thus be written as

$$\Delta S_S = \Delta H_R/T + R \ln P_{ins} \quad (4)$$

Using eqs 3 and 4, we obtain $\Delta G_S = \Delta H_S - T\Delta S_S = \Delta H_B - R \ln P_{ins}$. Thus, the enthalpy−entropy compensating part ($\Delta S_R = \Delta H_R/T$) has no effect on ΔG_S. The excluded volume entropy reflects the reduction of the solvent entropy due to presence of a cavity that excludes some of the volume available to the solvent. Hence, P_{ins} decreases with increasing penetrant size. We shall not further discuss the sorption entropy at this point and refer the reader to refs 6−9 for further details. Using the relation between ΔG_S and the gas solubility S, given by eq 1, we obtain $S \sim P_{ins} \exp[-\Delta H_B/RT]$; i.e., the gas solubility depends on the excluded volume entropy and on the penetrant binding enthalpy. Importantly, the solubility S does not depend on ΔH_R. Therefore, ΔH_S (see eq 2) does not fix the magnitude of S, and it may be misleading to use ΔH_S as a measure of polymer-penetrant interaction to rationalize variations in gas solubility among a series of gas penetrants. This will in particular be the case

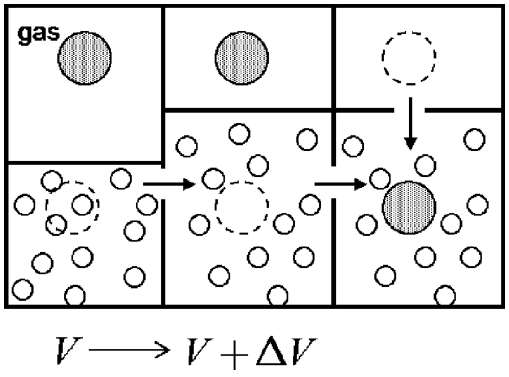

Figure 1. Two-step thermodynamic process for gas solubility in liquids at constant pressure and temperature. In the first step from the left, a molecular sized cavity is created which reduces the cohesive forces between the solvent molecules in contact with the cavity. The corresponding enthalpy change is ΔH_R. The volume change is ΔV. In the second step, the penetrant gas is introduced into the empty cavity. The corresponding enthalpy change is ΔH_B. It is assumed that rearrangement of solvent molecules occurs in the first step only. Physically, this assumption is meaningful for nonpolar gases interacting with the solvent through (weak) van der Waals forces.

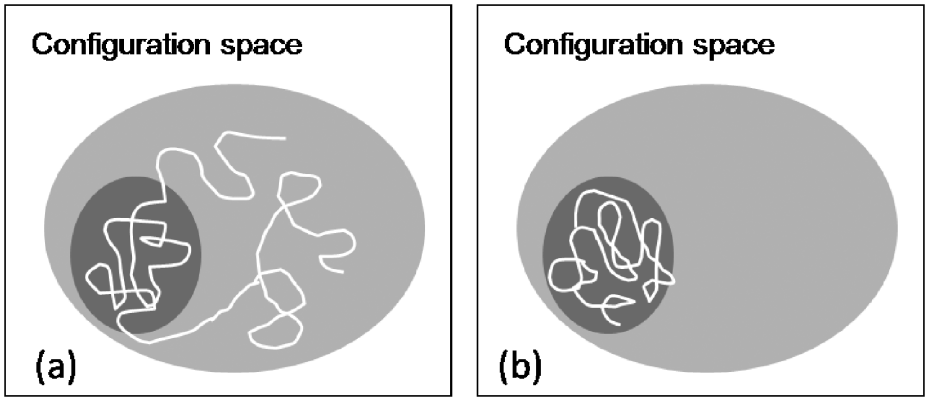

Figure 2. Schematic representation of the solvent configuration space. Each oval represents a set of molecular arrangements (configurations). The lighter gray area represents the "important" configuration space area of the pure solvent system; i.e., it contributes to, e.g., 99.9% of the corresponding partition function. The darker gray area corresponds to those configurations in which the dashed stencil in the middle part of Figure 1 is devoid of solvent molecules. The line connects configurations visited by the system during a finite time interval; i.e., it shows a pathway along which the system explores its configuration space during the course of a finite observation time. (a) Solvent configuration space before solute insertion. (b) Solvent configuration space after solute insertion. In part a, enthalpy and entropy fluctuations upon sampling of the darker gray are exactly compensating: $\Delta H_R = T\Delta S_R$. In part b, solute insertion confines the solvent to sampling a smaller region in configuration space.

when the absolute magnitudes of ΔH_R and ΔH_B are comparable and strongly gas dependent.

The Reorganization Enthalpy. We shall now seek to express ΔH_R in terms of macroscopic quantities that are available from experiments. We assume that the system is at constant pressure P and temperature T. Figure 1 shows that the cavity formation step causes a fluid volume increment ΔV.[11] Hence, a first (trivial) contribution to ΔH_R is the pressure-volume work $P\Delta V$, which in liquids is usually negligible.[6] The difference in cohesive forces between solvent molecules before and after the cavity formation step determines the magnitude of ΔH_R. Because the system is at constant pressure, solvent molecules far away from the cavity necessarily remain in an identical thermodynamic state before and after introduction of the solute. Therefore, ΔH_R may be interpreted as the enthalpy of solvent molecules in a microscopic region centered around the cavity, *excess* to the enthalpy of the solvent molecules in the bulk. Although ΔH_R is the enthalpy change of the overall fluid system, it is not equally spread over all solvent molecules in the system but is localized. Using similar arguments, ΔV represents a local reduction of the fluid density rather than a nonlocal one (*i.e.*, ΔV is *not* spread over all solvent molecules of the system). A thermodynamic measure for the magnitude of the intermolecular forces operating between molecules of the solvent is provided by the energy-volume coefficient—or "internal pressure"—$(\partial U/\partial V)_T$. This quantity relates the susceptibility of the internal energy to isothermal volume change. We now assume that the process of cavity formation corresponds to a local expansion ΔV of the solvent with a corresponding enthalpy change given by

$$\Delta H_R \cong \left[\left(\frac{\partial U}{\partial V}\right)_T + P\right]\Delta V = T(\alpha_P/\kappa_T)\Delta V \qquad (5)$$

In eq 5, α_P is the thermal expansion coefficient of the liquid solvent, and κ_T is the liquid solvent isothermal compressibility. All quantities on the right-hand-side of eq 5 are macroscopic system properties that can be obtained from polymer PVT data and (sorption induced) dilation experiments.

Once ΔH_S and ΔH_R have been determined from experimental data based on eqs 2 and 5, respectively, ΔH_B can be obtained from eq 3. If, furthermore, ΔG_S is determined from the measured solubility according to eq 1, the sorption entropy can be obtained from $\Delta S_S = (\Delta H_S - \Delta G_S)/T$. Finally, the insertion probability, P_{ins}, follows from eq 4. When gas sorption data are analyzed in this way, a full thermodynamic characterization of penetrant sorption is obtained, which provides access to the newly introduced quantities P_{ins} and ΔH_B, which, as described above, characterize the molecular-scale processes depicted in Figure 1.

The above reasoning, used to arrive at eq 5, is certainly rather sketchy, and it is not a priori clear if macroscopic system properties can be used to describe a *local* expansion process. However, eq 5 can alternatively be obtained from statistical mechanics theories of liquids.[4,12−14] The relation between cavity formation and the solvent internal pressure has been observed in early experimental work on hydrogen gas solubility in dimethyl sulfoxide (DMSO) − water systems.[15] Recently reported molecular simulations indicate that the assumptions required to arrive at eq 5 introduce relative deviations from the true reorganization enthalpy (obtained from simulation) smaller than 1% for permanent gases and smaller than 10% for hydrocarbons up to butane in liquid hexane,[5] liquid DMSO,[5] and aqueous DMSO solutions.[16] These deviations become significantly smaller when the application of eq 5 is restricted to nonpolar solvents.[4,5] Equations 3 and 5 are, therefore, expected to provide reliable, new data regarding the thermodynamics of gas sorption in polymers. This will be illustrated based on the example discussed below.

Table 1. Light Gas, Hydrocarbon, and Perfluorocarbon Sorption Enthalpies (ΔH_S), Partial Molar Volumes (ΔV_S), Reorganization Enthalpies (ΔH_R), and Binding Enthalpies (ΔH_B) in PDMS

	ΔH_S (kJ/mol)	ΔV_S (cm^3/mol)	ΔH_R (kJ/mol)	ΔH_B (kJ/mol)
He	6.7[a]	26[e]	6.0	0.7
Ne	5.2[a]	28[e]	6.4	−1.2
Ar	−0.9[a]	47[e]	10.8	−11.7
Kr	−5.8[a]	51[e]	11.7	−17.5
Xe	−10.7[a]	59[e]	13.6	−24.3
H_2	4.4[a]	34[e]	7.8	−3.4
N_2	−0.3[a]	54[e]/64[f]	12.4/16.4	−12.7/−16.7
O_2	−0.4[a]	46[e]/48[f]	10.6/12.3	−11.0/−12.7
CO_2	−12.1[b]	50[e]/48[f]	11.5/12.3	−23.6/−24.4
CH_4	−5.8[c]	54[e]/57[f]	12.4/14.6	−18.2/−20.4
C_2H_6		70[e]/73[f]	16.1/18.7	
C_3H_8	−20[d]	85[e]/91[f]	19.6/23.3	−39.6/−43.3
n-C_4H_{10}	−23[c]	101[e]/110[f]	23.3/28.1	−46.3/−51.1
CF_4	−6.5[g]	87[e]/86[f]	20.0/22.0	−26.5/−28.5
C_2F_6	−9.1[g]	119[e]/139[f]	27.4/35.6	−36.5/−44.7
C_3F_8	−13[d]	149[e]/173[f]	34.3/44.3	−47.3/−57.3

[a] Reference 22. [b] Reference 23. [c] Reference 19. [d] Reference 20 [e] Reference 24. [f] Reference 21. [g] This work.

2. Analysis of Experimental Data

Sorption of Permanent Gases, Hydrocarbons, and Their Fluorocarbon Analogues in PDMS. In this section, we shall use the formalism developed above to analyze enthalpies of gas sorption in poly(dimethylsiloxane) (PDMS). In addition to light gases, we analyze the available data on hydrocarbons and their fluorocarbon analogues, whose energetic interactions with PDMS are believed to differ strongly. Merkel et al.[17,18] reported hydrocarbon and perfluorocarbon gas solubilities in PDMS. In contrast to hydrocarbons, perfluorocarbons are sparingly soluble in PDMS and exhibit linear sorption isotherms. Exceptionally low fluorocarbon solubilities in PDMS were ascribed to poor penetrant/polymer energetic interactions.[17] Here, we analyze hydrocarbon and perfluorocarbon gas solubilities in PDMS using the following expression based on eqs 3 and 5

$$\Delta H_S \cong T(\alpha_P/\kappa_T)\Delta V + \Delta H_B \qquad (6)$$

The gas sorption enthalpies ΔH_S and partial molar volumes ΔV were taken from refs 19−24. Sorption enthalpies of CF_4 and C_2F_6 in PDMS were obtained from temperature dependent sorption measurements further described in the Appendix. The PDMS isobaric thermal expansion coefficient, $9.1 \times 10^{-4}\ K^{-1}$, and isothermal compressibility, 1.06×10^{-4} atm^{-1}were taken from ref 19 and were used together with the partial molar volumes given in ref 21 in order to calculate ΔH_R. The partial molar volumes from ref 24 were combined with the PDMS isobaric thermal expansion coefficient, $7.7 \times 10^{-4}\ K^{-1}$, and isothermal compressibility, 9.9×10^{-5} atm^{-1}, given in the same reference. Table 1 summarizes the data obtained from the analysis based on eqs 5 and 6 in which we used $T = 298$ K. In addition to the hydrocarbons and perfluorocarbons mentioned above, we included available data for noble and light gases.[22−24] It should be noted that the fluorocarbon partial molar volumes are significantly larger than those of the corresponding hydrocarbons. Hence, the reorganization enthalpies $T(\alpha_P/\kappa_T)\Delta V$ are significantly

Table 2. Binding Enthalpies $\Delta H_B^\bullet(T)$ of Pure Fluid Alkanes and Perfluoroalkanes at Different Temperatures T Compiled from Ref 25

	T (K)	$\Delta H_{vap}(T)$ (kJ/mol)	$\Delta H_B^\bullet(T)$ (kJ/mol)
CH_4	99.5	8.5	−17.0
C_2H_6	184.1	14.7	−29.4
C_3H_8	231.0	18.8	−37.6
n-C_4H_{10}	272.1	22.4	−44.8
CF_4	145.1	11.8	−23.6
C_2F_6	194.9	16.2	−32.4
C_3F_8	236.4	19.8	−39.6

larger, too. Application of eq 6 reveals that the binding enthalpies of the fluorocarbons are in all cases significantly more negative than that of their hydrocarbon analogues. Hence, the fluorocarbon-PDMS interactions are in all cases *stronger* than the corresponding hydrocarbon−PDMS interactions. Because a fluorocarbon is bigger, it will have a larger electronic polarizability than its hydrocarbon analogue resulting in stronger van der Waals interactions with the matrix polymer.

The magnitude of the penetrant binding enthalpy in PDMS can be compared with the binding enthalpy of the penetrant in its own liquid. The latter enthalpy, which we refer to as $\Delta H_B^\bullet$, corresponds to the second step in Figure 1 in a self-solvation process (*e.g.*, the binding enthalpy of propane in liquid propane). Assuming that the interactions in the liquid are pairwise additive, we can write $\Delta H_B^\bullet = -2\Delta H_{vap}$,[6] where ΔH_{vap} is the heat of vaporization of the liquid. The binding enthalpies of alkanes and fluoroalkanes in their own liquids are listed in Table 2.[25] Hydrocarbon and fluorocarbon penetrants bind more strongly with the PDMS matrix than with their own liquids. The differences are bigger for the fluorocarbon penetrants. We note that the relation between the quantities discussed here and the more familiar mixing enthalpies used in the literature[20] is given by $\Delta H_S = \Delta H_{cond} + \Delta H_{mix} = \Delta H_R + \Delta H_B$. Hence, it follows that $\Delta H_{mix} = \Delta H_R - \Delta H_{cond} + \Delta H_B$. Therefore, the difference between the penetrant binding enthalpy to its own liquid and to the PDMS matrix should not be confused with the mixing enthalpy which contains compensating contributions that do not affect solubility.

Figure 3a shows the correlation between the binding enthalpy and the penetrant critical temperature T_C. The fluorocarbon data (open symbols) fall below those of other penetrants (filled symbols) with comparable T_C. Note that we included two data points for those penetrants where partial molar volumes in PDMS have been reported in two independent studies (refs 21 and 24). The data in Figure 3a indicate that the fluorocarbons follow a correlation with T_C similar to the other penetrants but shifted downward to more favorable binding enthalpies. The results clearly indicate that low fluorocarbon solubilities cannot be explained in terms of weak polymer−penetrant interaction.

Figure 3b shows the correlation between the penetrant binding enthalpy and the gas critical volume V_C. The critical volume is a measure of penetrant's molecular size. Because we anticipate the penetrant's binding enthalpy to be proportional to its electronic polarizability (which in turn is proportional to the penetrant's molecular volume), we believe that the correlation between ΔH_B and V_C is physically meaningful. Moreover, if we compare fluorocarbons and hydrocarbons *of the same size*, the excluded volume entropies are approximately the same and the difference in observed solubilities will be determined by differences in the binding enthalpies only. Figure 3b indicates that fluorocarbons interact with PDMS equally strong than (hypothetical) hydrocarbons of the same size. Note, however, that some

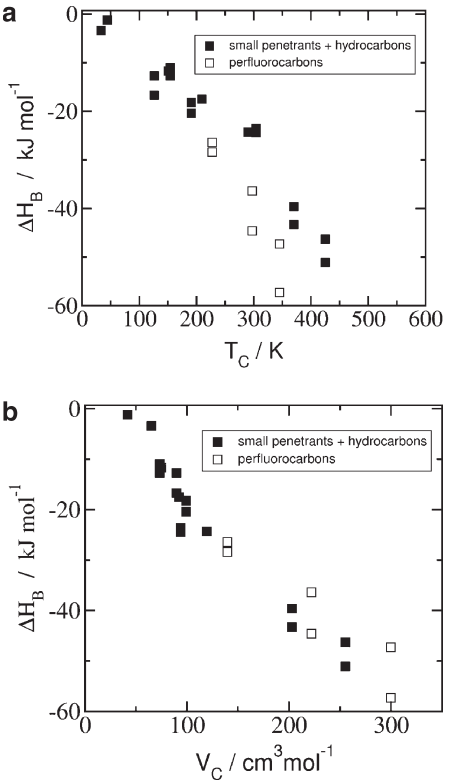

Figure 3. (a) Correlation between the penetrant binding enthalpy in PDMS and gas critical temperature and (b) between the penetrant binding enthalpy in PDMS and the gas critical volume. Filled symbols: noble gases, light gases and hydrocarbons. Open symbols: perfluorocarbons.

caution has to be taken here, because partial molar volumes reported in the literature[21,24] differ quite substantially for the larger penetrants studied in this work. This causes an uncertainty in the fluoropropane binding enthalpy of 10 kJ/mol.

On the basis of the discussion above, we conclude that low fluorocarbon over hydrocarbon solubilities do not result from weak fluorocarbon-PDMS interactions, as suggested before.[17,18] On the contrary, a fluorocarbon has a stronger binding interaction with the PDMS matrix than the corresponding hydrocarbon. Fluorocarbons however occupy larger holes in the liquid matrix because they are bigger; thermodynamically this is penalized by an unfavorable excluded volume entropy which acts to reduce solubility. Lower fluorocarbon solubilities are therefore explained by a more unfavorable balance between the penetrant binding enthalpy (which favors solubility) and excluded volume entropy (which opposes solubility).

3. Why Does Solubility Usually Scale Quite Well with T_c?

The solubility of penetrants whose interaction with polymer matrices is dominated by van der Waals forces usually correlates quite well with the penetrant critical temperature, T_C. Although phenomenological macroscopic explanations of this observation are available in the literature,[26−28] explanations based on a microscopic (molecular scale) picture have not been provided so far. Microscopically, one pictures gas molecules impinging on the interface with the liquid. This happens, at first only from above and then also from below, until the fluxes into and out off the liquid phase have reached a dynamic equilibrium. Because a gas molecule impinging on the interface will in general not have sufficient kinetic energy to displace a liquid molecule—in other words, a gas molecule cannot dig its own hole—it can only enter a

microscopic cavity in the fluid. This picture is schematically expressed in Figure 1. Gas solubility will be larger, the larger the probability P_{ins} that a cavity of the appropriate size is found somewhere in the liquid phase. Hence, the gas solubility S is proportional to the insertion probability: $S \sim P_{ins}$ (we recall that $S \sim P_{ins} \exp[-\Delta H_B/RT]$). Because P_{ins} decays exponentially with cavity size,[12,13] we assume that $P_{ins} \sim \exp[-aV_C]$ (where a is a positive constant and V_C is the gas critical volume, which we here take as a measure of the penetrant volume). In addition to this entropic aspect of penetrant solubility, we now evaluate the penetrant binding enthalpy ΔH_B, which affects S according to $S \sim P_{ins} \exp[-\Delta H_B/RT]$. Since we have limited ourselves to polymer-penetrant interactions dominated by dispersion forces, ΔH_B is determined by the penetrant's electronic polarizability. The electronic polarizability is proportional to the van der Waals volume of the penetrant, which in turn correlates with the penetrant gas critical volume V_C. Hence, we find $\exp[-\Delta H_B/RT] \sim \exp[bV_C]$ (note that usually $\Delta H_B < 0$, hence $-\Delta H_B \sim V_C$; b is a positive constant). We, therefore, arrive at the result $\log S \sim (b - a)V_C$. This result follows straightforwardly from the microscopic description used in this work and cannot easily be obtained by alternative approaches. The final step required to arrive at $\log S \sim T_C$ is straightforward. The electronic polarizability of nonpolar penetrants (which is proportional to V_C) also determines the strength of penetrant-penetrant interactions in the gas phase, which in turn affect the penetrant's condensability and T_C. Hence, we may write $V_C \sim T_C$ and, therefore, $\log S \sim (b - a)\ V_C \sim (c_E - c_S)\ T_C \sim T_C$ (c_E and c_S are two positive constants). By plotting the critical volumes of the small penetrant gases and hydrocarbons (up to *n*-butane) considered in this work versus their critical temperatures, we actually find that a quadratic fit of the data, $V_C \sim T_C^2$, provides a better description than a linear fit. This suggest that an alternative correlation $\log S \sim T_C^2$ exists, which has indeed been observed experimentally.[18,20,23,27,28]

It is due to the frequently observed correlation $\log S \sim T_C$ that solubility is usually being discussed in terms of polymer−penetrant interactions only. Indeed, T_C depends only on the energy parameter ε for Lennard-Jones fluids; hence, it is quite natural to refer to the nature of the polymer-penetrant interactions when deviations from the above correlation are observed. The merit of the above microscopic treatment is that it reminds us that the observed proportionality arises from two *opposing* dependencies on T_C. The entropic dependency $-c_S T_C$ *opposes* solubility (larger penetrants require larger cavities), while the enthalpic dependency $c_E T_C$ *favors* solubility (polymer−penetrant dispersion forces are stronger for larger penetrants). Deviations from the correlation between S and T_C can quite easily be explained based on the microscopic treatment described in this work. For example, fluorocarbons have been found to not follow the correlation obtained for small penetrant gases and hydrocarbon gases in PDMS.[21] On the basis of the microscopic treatment developed in this paper, the deviation could be ascribed to the fact that fluorocarbons occupy larger cavities at the expense of a larger entropy penalty compared to the corresponding hydrocarbons.

We finally note that for glassy polymers similar arguments apply to arrive at the correlation between the solubility and T_C. If we consider a glassy matrix as an amorphous solid with a liquid like, yet frozen, microscopic structure, the same correlations as in the liquid state can be applied between $P_{ins}/\Delta H_B$ and V_C that lead to the well-known correlation between penetrant solubility and penetrant critical temperature. In glasses, the quantity P_{ins} corresponds with the penetrant accessible fractional free volume. Although eqs 4-6 cannot be applied to glassy polymers, eqs 1−3 may still be used, if it assumed that penetrant-induced non-equilibrium relaxations of the glassy matrix are absent. The penetrant binding enthalpy ΔH_B may then be approximated in the penetrant infinite dilute solubility limit where it is assumed that $\Delta H_R \simeq 0$ and, therefore, $\Delta H_S \simeq \Delta H_B$ (cf. Equation 3). Finally, the penetrant accessible fractional free volume P_{ins} is obtained from the penetrant infinite dilute solubility $S(P = 0)$ and ΔH_B using the relation $S(P = 0) = (T_0/TP_0) \times P_{ins} \exp[-\Delta H_B/RT]$ ($T_0 = 273.15$ K and $P_0 = 1$ atm).

4. Conclusions

In this paper, we have described a two-step molecular sorption process (Figure 1) for nonpolar penetrants in liquidlike polymer matrices. The enthalpic contributions to this process, corresponding to polymer reorganization and polymer−penetrant binding (eq 3), can be estimated from experimental sorption data (sorption enthalpy and partial molar volume) provided that the pure polymer's isobaric thermal expansion coefficient and isothermal compressibility are available. The ideas are based on earlier concepts applied to gas solubility in liquids and apply to polymer/penetrant systems at temperatures above T_G. We have re-emphasized an exact rule of enthalpy−entropy compensation based upon which it can be shown that the *binding enthalpy* determines gas solubility while the reorganization enthalpy has no effect on it. We anticipate that future analysis of the *binding enthalpy* will establish new correlations between the molecular properties of the polymer and penetrant which will benefit our understanding of the sorption thermodynamics of polymer/penetrant systems. We have furthermore shown that the frequently observed correlation $\log S \sim T_C$ or $\log S \sim T_C^2$ follows from the microscopic context (Figure 1) used in this paper while deviations from it can be traced back to molecular properties. The arguments used to arrive at these correlations are equally valid for both rubbery and glassy polymer matrices.

Appendix. Experimental Determination of CF_4 and C_2F_6 Solubility in PDMS

Polydimethylsiloxane (PDMS) dense films were prepared in a similar manner as ref 19. Dehesive 940A (Wacker Silicones Corporation, Adrian, MI) was mixed with cyclohexane (Sigma-Aldrich Chemical Co., Milwaukee, WI), making a 40% solution. Before casting, a proprietary cross-linker (V24) and catalyst (OL) system provided by Wacker was added to the polymer solution. Films were prepared by pouring the polymer solution into a casting ring on a Teflon-coated glass plate, which was dried slowly under ambient conditions for 4 days. Residual solvent was removed by heating the resulting film in an oven at 110 °C for 30 min. Finally, the films were washed with *n*-heptane in a Soxhlet extractor for 3 days to remove any unreacted cross-linker, catalyst and unbound polymer.

Semiconductor 3N5 grade (99.95%) tetrafluoromethane and hexafluoroethane were purchased from Matheson Tri-Gas (Basking Ridge, NJ). Both gases were used as received.

Pure gas solubility coefficients were determined using a three-chambered barometric pressure-decay apparatus described in previous publications.[19,29] Each chamber was equipped with a SuperTJE pressure transducer (Honeywell Sensotec, Columbus, OH) which had an accuracy of 0.05% full scale. The cell volumes were determined by the Burnett expansion method.[30] For the experiments reported in this paper, only two volumes were utilized: an empty charge chamber, and a chamber containing the PDMS sample.[19] The temperature range of these experiments was −20 to +35 °C. The desired temperatures were maintained by immersion of the apparatus in a controlled temperature bath using either water or ethanol as the bath fluid. The PDMS sample was degassed by maintaining the sorption system under vacuum overnight before each experiment. Initially, a desired amount of penetrant gas was added to the charge volume. After a steady pressure reading was obtained, the penetrant gas was expanded into the sample chamber and allowed to equilibrate. The amount

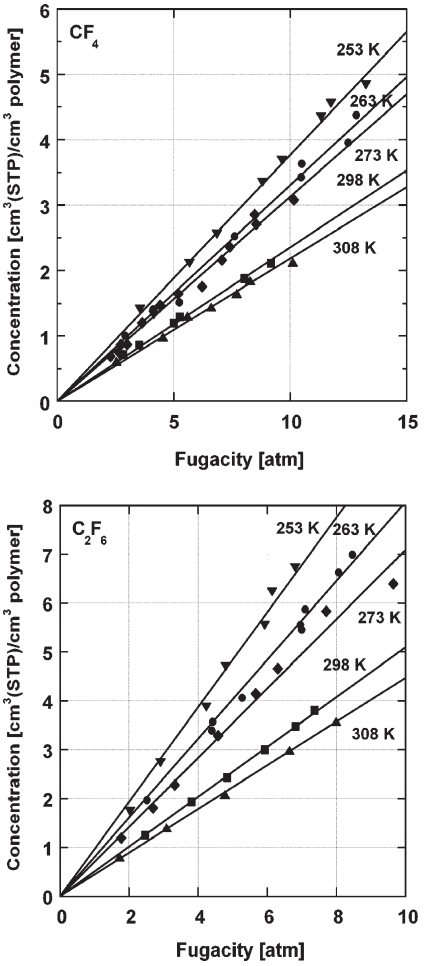

Figure 4. (a) CF_4 and (b) C_2F_6 pure gas sorption isotherms in PDMS as a function of fugacity. The experiment temperatures are as follows: (▲) 308 K; (■) 298 K; (◆) 273 K; (●) 263 K; (▼) 253 K. The lines represent the least-squares linear fit.

of gas sorbed in the polymer as a function of penetrant fugacity was determined using mass balance calculation. Once the pressure in the sample chamber was constant, additional penetrant can be admitted into the charge chamber and then expanded into the sample chamber to establish another equilibrium, thus incrementally increasing the amount of gas sorbed in the polymer.

The gas solubility in the polymer can be determined as follows:[31]

$$S_A = \frac{C_A}{f} \tag{7}$$

where C_A is the concentration of gas A sorbed in the polymer per unit volume of penetrant-free polymer when the fugacity of the gas phase in contact with the polymer is f. Fugacity is used to account for gas phase nonidealities, especially in the case of C_2F_6 at lower temperatures. The Soave−Redlich−Kwong (SRK) equation of state is used to estimate fugacity.[19,32]

The sorption isotherms of CF_4 and C_2H_6 are plotted in Figure 4. As noted in the main body of this paper, the equilibrium concentration of these gases at a particular fugacity are much lower than that of their respective hydrocarbon counterparts (i.e., CH_4 and C_2H_6).[18,20] Consequently, these sorption isotherms are linear. In contrast, while CH_4 sorption isotherms in PDMS are linear,[19] the C_2H_6 sorption isotherms are nonlinear and convex to the fugacity axis.[18] This behavior is similar to the contrast

Table 3. Solubility Coefficients of CF_4 and C_2F_6 in PDMS as given by Eq 7

T (K)	S_{CF_4} (cm^3(STP)/cm^3 polymer atm)	$S_{C_2F_6}$ (cm^3(STP)/cm^3 polymer atm)
253	0.38	0.97
263	0.33	0.81
273	0.31	0.71
298	0.23	0.51
308	0.22	0.45

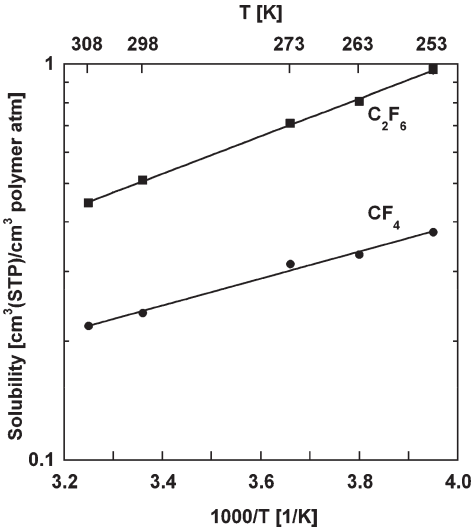

Figure 5. Solubility coefficients of (●) CF_4 and (■) C_2F_6 in PDMS plotted against temperature. The lines represent the least-squares exponential fit.

between the sorption isotherms of C_3H_8 and C_3F_8.[20] The CF_4 and C_2F_6 sorption isotherms at 308 K (i.e., 35 °C) are comparable to those obtained in refs 18 and 21.

On the basis of the linear regression results of the sorption isotherms (which are modeled using Henry's law), the solubility coefficients are estimated in Table 3. The enthalpy of sorption can be calculated from these solubility coefficients as follows:[19]

$$-\frac{\Delta H_S}{R} = \left(\frac{d(\ln S_A)}{d(1/T)}\right) \tag{8}$$

The enthalpy of sorption is calculated by least-squares fit of the natural logarithm of solubility coefficients against inverse temperature, as given in Figure 5. $-\Delta H_S/R$ is obtained in unit of K. The fits yield ΔH_S values of −6.5 kJ/mol and −9.1 kJ/mol for CF_4 and C_2F_6, respectively (cf. Table 1).

References and Notes

(1) van der Vegt, N. F. A. *J. Membr. Sci.* **2002**, *205*, 125–139.
(2) Ghosal, K.; Freeman, B. D. *Polym. Adv. Technol.* **1994**, *5*, 673–697.
(3) In this paper, we limit ourselves to the infinite dilution limit. Hence, interactions between dissolved penetrant molecules are ignored in our further discussion of ΔH_S. At the corresponding, low pressure, the gas phase is furthermore assumed to behave ideally. Hence, ΔH_S does not contain gas phase contributions.
(4) Ben-Amotz, D.; Raineri, F. O.; Stell, G. *J. Phys. Chem. B* **2005**, *109*, 6866–6878.
(5) Peter, C.; van der Vegt, N. F. A. *J. Phys. Chem. B* **2007**, *111*, 7836–7842.
(6) Ben-Naim, A. *Molecular Theories of Solutions*; Oxford University Press: New York, 2006. Ben-Naim, A. *Molecular Theory of Water and Aqueous Solutions*; World Scientific: Singapore, 2009.
(7) Ben-Naim, A. *Biopolymers* **1975**, *14*, 1337–1355.
(8) Yu, H.-A.; Karplus, M. *J. Chem. Phys.* **1988**, *89*, 2366–2379.

(9) Sanchez, I. C.; Truskett, T. M.; In 't Veld, P. J. *J. Phys. Chem. B* **1999**, *103*, 5106.
(10) P_{ins} is defined as the probability that a solute, randomly inserted in the pure liquid solvent, finds all solvent molecules properly positioned and oriented to accommodate all chemical moieties of the solute.
(11) The volume increment ΔV and the penetrant partial molar volume ΔV_S are related according to $\Delta V = \Delta V_S - RT\kappa_T$. The quantity $RT\kappa_T$ (with κ_T being the solvent phase isothermal compressibility) is subtracted from the partial molar volume to account for the assumption that the cavity is formed at an arbitrary but *fixed* position in the system.[6] Hence, also the solute is introduced at a fixed position. For further details; see ref 6. In this work, we will ignore the difference between ΔV and ΔV_S because $RT\kappa_T \approx 2.6$ cm^3/mol, which is small compared to the experimental uncertainties in ΔV_S.
(12) Reiss, H. *Adv. Chem. Phys.* **1966**, *9*, 1–84.
(13) Pierotti, R. A. *Chem. Rev.* **1976**, *6*, 717–726.
(14) Lee, B. *Biopolymers* **1985**, *24*, 813–823.
(15) Symons, E. A. *Can. J. Chem.* **1971**, *49*, 3940–3947.
(16) Ozal, T. A.; van der Vegt, N. F. A. *J. Phys. Chem. B* **2006**, *110*, 12104–12112.
(17) Merkel, T. C.; Bondar, V.; Nagai, K.; Freeman, B. D. *Macromolecules* **1999**, *32*, 370–374.
(18) Merkel, T. C.; Bondar, V. I.; Nagai, K.; Freeman, B. D.; Pinnau, I. *J. Polym. Sci., Polym. Phys. Ed.* **2000**, *38*, 415–434.
(19) Raharjo, R. D.; Freeman, B. D.; Sanders, E. S. *J. Membr. Sci.* **2007**, *292*, 45–61.
(20) Prabhakar, R. S.; Merkel, T. C.; Freeman, B. D.; Imizu, T. I.; Higuchi, A. *Macromolecules* **2005**, *38*, 1899–1910.
(21) De Angelis, M. G.; Merkel, T. C.; Bondar, V. I.; Freeman, B. D.; Doghieri, F.; Sarti, G. C. *J. Polym. Sci., Polym. Phys. Ed.* **1999**, *37*, 3011–3026.
(22) Barrer, R. M.; Chio, H. T. *J. Polym. Sci. C* **1965**, *10*, 111–138.
(23) Shah, V. M.; Hardy, B. J.; Stern, S. A. *J. Polym. Sci., Polym. Phys. Ed.* **1986**, *24*, 2033–2047.
(24) Kamiya, Y.; Naito, Y.; Terada, K.; Mizoguchi, K.; Tsuboi, A. *Macromolecules* **2000**, *33*, 3111–3119.
(25) NIST Chemistry WebBook. http://webbook.nist.gov/chemistry
(26) Michaels, A. S.; Bixler, H. J. *J. Polym. Sci.* **1961**, *L*, 393–412.
(27) Stern, S. A.; Mullhaupt, J. T.; Gareis, P. J. *AIChE J.* **1969**, *15*, 64–73.
(28) Suwandi, M. S.; Stern, S. A. *J. Polym. Sci.* **1973**, *11*, 663–681.
(29) Ribeiro, C. P.Jr.; Freeman, B. D. *Macromolecules* **2008**, *41*, 9458–9468.
(30) Burnett, E. S. *J. Appl. Mech.* **1936**, *3*, 136–140.
(31) Petropoulos, J. H. In *Polymeric Gas Separation Membranes*; Paul, D. R., Yampolskii, Yu. P., Eds.; CRC Press: Boca Raton, FL, 1994.
(32) Poling, B. E.; Prausnitz, J. M.; O'Connell, J. P. *The Properties of Gases and Liquids*, 5th ed.; McGraw-Hill: New York, 2001.